Article

Excess Electron Attachment Induces Barrier-Free Proton Transfer in Binary Complexes of Uracil with HSe and HS but Not with HO

Maciej Haraczyk, Rafa Bachorz, Janusz Rak, Maciej Gutowski,
Dunja Radisic, Sarah T. Stokes, J. Michael Nilles, and Kit H. Bowen

More About This Article

Additional resources and features associated with this article are available within the HTML version:

- Supporting Information
- Links to the 8 articles that cite this article, as of the time of this article download
- Access to high resolution figures
- Links to articles and content related to this article
- Copyright permission to reproduce figures and/or text from this article

View the Full Text HTML

Excess Electron Attachment Induces Barrier-Free Proton Transfer in Binary Complexes of Uracil with H$_2$Se and H$_2$S but Not with H$_2$O

Maciej Harańczyk,[†,‡] Rafał Bachorz,[‡,§] Janusz Rak,[‡] and Maciej Gutowski*,[†]

Chemical Sciences Division, Pacific Northwest National Labolatory, Richland, Washington 99352,
Department of Chemistry, University of Gdansk, Sobieskiego 18, 80-952 Gdansk, Poland, and
Department of Chemistry, Quantum Chemistry Group, Adam Mickiewicz University, Poznan, Poland

Dunja Radisic, Sarah T. Stokes, J. Michael Nilles, and Kit H. Bowen, Jr.*

Department of Chemistry, Johns Hopkins University, Baltimore, Maryland 21218

Received: March 12, 2003

The photoelectron spectrum of the uracil−H$_2$S anionic complex (UH$_2$S)$^-$ has been recorded with 2.540 eV photons. Unlike the (uracil−H$_2$O)$^-$ spectrum, which displays a broad feature with maximum at about 0.9 eV, the (UH$_2$S)$^-$ spectrum reveals a broad feature with a maximum between 1.7 and 2.1 eV. The latter vertical detachment energy value is too large to be attributed to an (UH$_2$S)$^-$ complex in which an intact uracil anion is solvated by H$_2$S. The effects of electron attachment to the UH$_2$A complexes (A = Se, S, O) have been studied at the density functional theory level with the B3LYP and MPW1K exchange correlation functionals as well as at the second-order Møller−Plesset perturbation theory level. The three acids cover a broad range of acidity with calculated gas-phase deprotonation enthalpies being equal to 14.8, 15.1, and 16.9 eV for H$_2$Se, H$_2$S, and H$_2$O, respectively. In the case of H$_2$Se and H$_2$S, electron attachment is predicted to induce a barrier-free proton transfer (BFPT) from the acid to the O8 atom of uracil, with the product being the radical of hydrogenated uracil bound to AH$^-$. No BFPT is predicted for the anion of uracil with H$_2$O. Critical factors for the occurrence of BFPT have been analyzed, and the role of the stabilizing interaction between the hydrogenated uracil and the deprotonated acid has been discussed. Four structures have been considered for every UH$_2$A complex, and their relative stabilities are different for the neutral and anionic species. The increased stabilities of anionic complexes that undergo BFPT can be related to the properties of the second hydrogen bond (C5H···A or N1(3)H···A). In comparison with the case of neutral structures, this bond is weakened for anionic structures without BFPT and strengthened for those with BFPT.

1. Introduction

Low-energy electrons are produced in large quantities by high-energy radiation interacting with condensed phases. They appear as secondary products of the radiolysis of water, with the primary products being the OH and H radicals.[1] In the past, the genotoxicity of radiation was studied mainly in the context of the OH and H radicals, and the relationship between their presence and DNA mutations is well documented.[2,3] Only in the past decade has it become clear that direct interactions with charged particles in a radiation field account for a significant fraction of the radiation damage to DNA in cells.[4] This reversal in traditional focus derives primarily from a reassessment of the radical-scavenging capacity of the intracellular medium; OH damage to DNA is limited to those radicals which were formed within a few nanometers of the DNA. Current estimates place direct damage at about one-third of the total.[5]

The recent experiments of Sanche and co-workers[1] suggest that electrons with energies 1−20 eV can induce DNA damage. However, in contrast to the case of reactions between genetic material and reactive compounds, such as OH radicals, alkylating and oxidizing agents, or halogens, low-energy electrons

directly trigger single- and double-strand breaks in DNA. The resonance structure of the damage quantum-yield versus incident electron energy[1] suggests that the process proceeds via temporary anionic states, probably localized on the nucleic acid base (NAB) molecules. Thus, anions of NABs are suspected to be the primary species responsible for DNA strand breaking due to excess electrons.

Negatively charged clusters of biologically important molecules have been extensively studied, both experimentally[6,7] and theoretically.[8−21] Electron trapping on nucleic acid bases has been an important topic in radiation biology for several decades. About 10 years ago, it was realized that the large polarities of NABs allow for the existence of dipole-bound anionic states as well.[8] While our recent CCSD(T) results indicate that the valence anionic state of uracil (U) is vertically stable with respect to the neutral by 0.507 eV,[22] our calculations also find the valence anonic state to be thermodynamically unstable by 0.215 eV with respect to the dipole-bound anionic state and by 0.147 eV with respect to the neutral.[22] The current view is that valence anionic states are unbound, or at best very weakly bound, for isolated NABs, but that they become dominant for solvated species.[23]

Intra- and intermolecular tautomerizations involving nucleic acid bases have long been suggested as critical steps in mutations of DNA.[24−26] Intramolecular proton-transfer reactions have been

---

† Pacific Northwest National Labolatory.
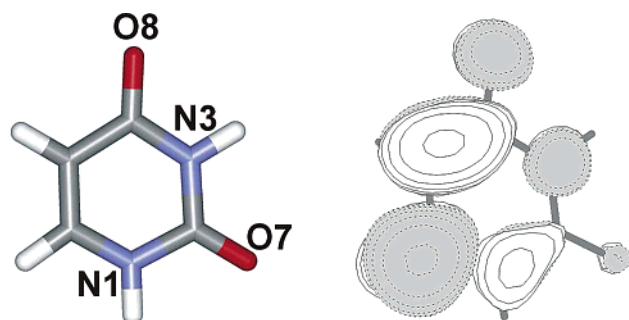‡ University of Gdansk.
§ Adam Mickiewicz University.

Figure 1. Numbering of atoms in uracil (left) and the singly occupied orbital for the anion of uracil in the valence π^* electronic state (right).

TABLE 1: Calculated Deprotonation Energy (E_{DP}), Entalphy (H_{DP}), and Gibbs Free Energy (G_{DP}) of H_2A[a]

acid	E_{DP}	H_{DP}	G_{DP}	H_{DP}^{exp}	G_{DP}^{exp}
H_2Se	14.955	14.780	14.506	14.800 ± 0.035[b]	14.536 ± 0.035[b]
H_2S	15.313	15.115	14.838	15.214 ± 0.125[c]	14.935 ± 0.135[c]
H_2O	17.155	16.859	16.555	16.942 ± 0.004[d]	16.656 ± 0.008[d]

[a] All results are in eV and are obtained at the B3LYP/6-31++G**(5d) level. [b] Reference 57. [c] Reference 58. [d] Reference 59.

studied for isolated and hydrated nucleic acid bases.[26–29,30] The intermolecular single and double proton-transfer reactions have been studied for the dimers of nucleic acid bases in both their ground and excited electronic states.[31–36] Only small activation barriers were found for the anionic and cationic GC pair, with the proton transfer reaction being favorable for the anion and slightly unfavorable for the cation.[36]

The results of our recent studies on anionic complexes of uracil with glycine,[22] alanine,[37] and formic acid[38] suggest that valence-type anions of NABs are susceptible to intermolecular proton transfer to the anionic base. A driving force for the proton transfer is to stabilize the excess electron on a π^* orbital of the anionic base (see Figure 1 for the numbering of atoms in uracil and the excess electron orbital in its valence π^* anionic state). Our results strongly suggested that the electron attachment to complexes of uracil with glycine, alanine, or formic acid leads to a barrier-free proton transfer (BFPT) from the carboxylic group of an acid (HOOCX) to the O8 atom of U with the products being a neutral radical of hydrogenated uracil (UH$^\bullet$) and an anion of the deprotonated acid:[22,37,38]

$$U \cdots HOOCX + e^- \rightarrow UH^\bullet \cdots (OOCX)^- \qquad (1)$$

This conclusion was drawn by comparing the results of photoelectron spectroscopic (PES) measurements and the results of ab initio calculations for the anionic uracil–HOOCX complexes.

BFPT (or proton transfer with a low kinetic barrier) induced by electron attachment may also take place in DNA. To elucidate the fate of primary anionic states generated in DNA irradiated with low-energy electrons, one therefore needs to determine factors governing the occurrence of proton transfer in complexes between anionic NABs and proton donors. In the current study we investigate the occurrence of BFPT as an outcome of the interplay between the deprotonation energy of a proton donor, the protonation energy of the anionic uracil, and the strength of intermolecular hydrogen bonds. As proton donors we chose a series of non-oxyacids H_2A (A = Se, S, O) with their calculated deprotonation enthalpies covering a broad range of 14.8–16.9 eV; see Table 1. Together, the results of our photoelectron spectroscopic experiments and quantum chemical calculations strongly suggest that the anionic dimer of uracil
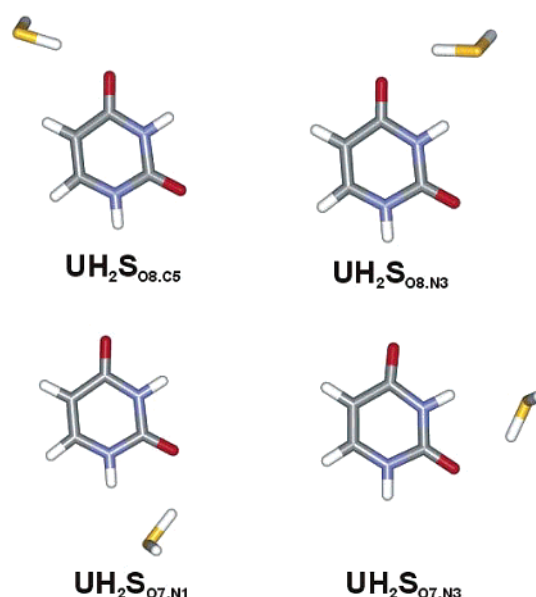

Figure 2. Neutral complexes of uracil and H_2S.

and H_2S undergoes BFPT. The same effect is predicted for H_2Se acting as a proton donor in the anionic complex with uracil, but not for H_2O. The anionic complex of uracil with H_2O is interpreted as being the anion of uracil in its valence π^* state solvated by H_2O.[7]

2. Methods

2.1. Experimental. Negative ion photoelectron spectroscopy is conducted by crossing a mass-selected beam of negative ions with a fixed-frequency laser beam and energy-analyzing the resultant photodetached electrons.[39] It is governed by the energy-conserving relationship: $h\nu = EBE + EKE$, where $h\nu$ is the photon energy, EBE is the electron binding energy, and EKE is the electron kinetic energy. One knows the photon energy of the experiment, one measures the electron kinetic energy spectrum, and then, by difference, one obtains electron binding energies, which in effect are the transition energies from the anion to the various energetically accessible states of its corresponding neutral.

Our apparatus has been described elsewhere.[40] To prepare the species of interest, uracil was placed in the stagnation chamber of a nozzle source and heated to ~180 °C. The expansion gas was a 5% H_2S/argon mixture. Its total pressure was 1–2 atm, and the nozzle diameter was 25 μm. Electrons were injected into the emerging jet expansion from a biased Th/Ir filament in the presence of an axial magnetic field. The resulting anions were extracted and mass-selected with a magnetic sector mass spectrometer. Electrons were then photodetached from the selected anions with ~100 circulating Watts of 2.540 eV photons and finally energy-analyzed with a hemispherical electron energy analyzer, having a resolution of 25 meV. We did not attempt to prepare (uracil–H_2Se)$^-$ due to the extreme toxicity of H_2Se.

2.2. Computational. The notations $UH_2A_{x,y}$ and $aUH_2A_{x,y}$ will be used for the neutral and anionic complexes of uracil (U) and an acid (A = O, S, or Se), respectively. The symbol x designates the particular oxygen atom of uracil which is involved in a hydrogen bond with H_2A, while the symbol y indicates the side of the oxygen atom involved in the hydrogen bond. Examples of this notation are presented in Figures 2 and 3.

The stability of the neutral (superscript = 0) or anionic (superscript = −) UH_2A complexes is expressed in terms of
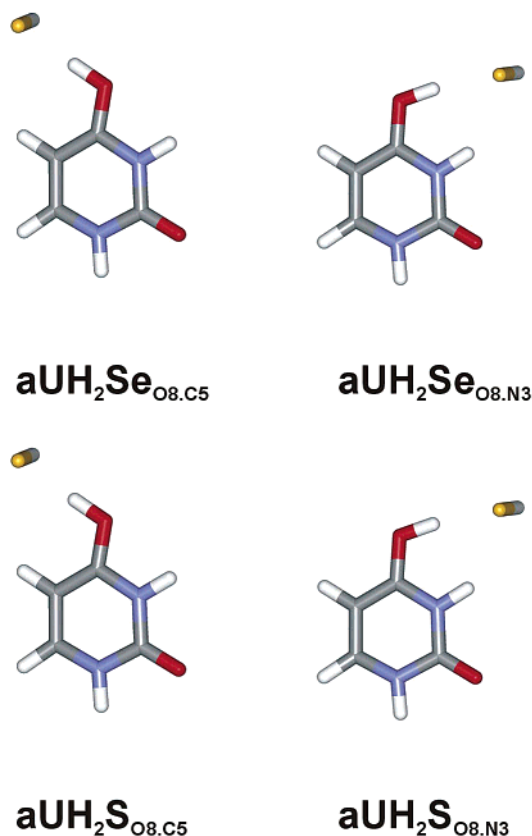
Effect of Electron Attachment on Proton Transfer

J. Phys. Chem. B, Vol. 107, No. 31, 2003 **7891**

Figure 3. Optimized structures of anionic complexes that underwent intermolecular barrier-free proton transfer.

Figure 4. Photoelectron spectra of the uracil–H_2O dimer anion (top), the uracil–H_2S dimer anion (middle), and the uracil–glycine dimer anion (bottom) recorded with 2.540 eV/photon.

E_{stab} and G_{stab}. E_{stab} is defined as the difference in the electronic energies of the monomers and the dimer

$$E_{stab} = E^{U^{(0,-)}}(\text{Geom}^{U^{(0,-)}}) + E^{H_2A}(\text{Geom}^{H_2A}) - E^{UH_2A^{(0,-)}}(\text{Geom}^{UH_2A^{(0,-)}}) \quad (2)$$

with the electronic energy E^X ($X = U^{(0-)}$, H_2A, or $UH_2A^{(0-)}$) computed for the coordinates determining the optimal geometry of X (i.e., the geometry where E^X is at the minimum). The values of E_{stab} were not corrected for basis set superposition errors because our earlier results demonstrated that the values of this error in B3LYP/6-31++G** calculations for a similar neutral uracil–glycine complex did not exceed 0.06 eV. The stabilization Gibbs energy, G_{stab}, results from supplementing E_{stab} with thermal contributions to energy from vibrations, rotations, and translations, pV terms, and the entropy term. The values of G_{stab} discussed below were obtained for $T = 298$ K and $p = 1$ atm, in the harmonic oscillator–rigid rotor approximation.

As our research method, we applied density functional theory (DFT)[41,42] with a Becke's three-parameter hybrid functional (B3LYP)[43−45] and a modified Perdew–Wang one-parameter method for kinetics (MPW1K) designed by Truhlar at al.[46] In both DFT approaches we used the same 6-31++G** basis set.[47,48] Five d functions were used on heavy atoms. The calculations of matrixes of second derivatives of energy (Hessians) were performed to confirm that final geometries were minima on potential energy surfaces.

The usefulness of the B3LYP/6-31++G** method to describe intra- and intermolecular hydrogen bonds has been demonstrated in recent studies through comparison with the second-order Møller–Plesset (MP2) predictions.[49−52] The ability of the B3LYP method to predict excess electron binding energies has recently been reviewed, and the results were found to be
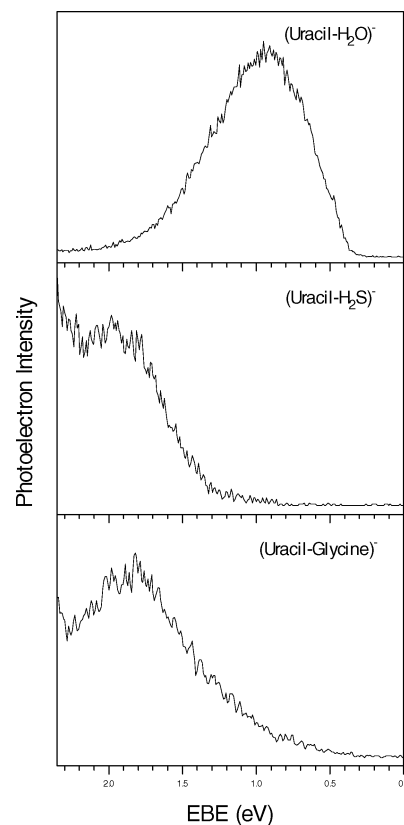
satisfactory for valence-type molecular anions.[53] We found that the value of the vertical detachment energy (VDE) determined at the B3LYP/6-31++G** level for the valence π^* anionic state of an isolated uracil is overestimated by 0.2 eV in comparison with the CCSD(T)/aug-cc-pVDZ result.[22] We will assume in the following that the same correction of 0.2 eV applies to the values of the VDE for all anionic UH_2A complexes in which an excess electron occupies a π^* orbital localized on uracil.

It is known that the B3LYP method underestimates barriers for proton-transfer reactions,[46] and thus, lack of a barrier for a proton-transfer reaction may be an artifact of the B3LYP method. For this reason, we performed additional geometry optimizations using a hybrid exchange-correlation potential MPW1K, which was parametrized to reproduce barrier heights for chemical reactions.[46] The MPW1K functional was optimized against a database of 40 barrier heights and 20 energies of reaction.[46,54] The performance of this functional for geometries of saddle points and barrier heights was found to be superior to that of the B3LYP functional as well as the second-order Møller–Plesset method.[46] Finally, a MP2 geometry optimization has been performed for one anionic ($aUH_2Se_{O7,N1}$) complex to verify the B3LYP and MPW1K predictions.

All calculations were carried out with the GAUSSIAN 98[55] code on a cluster of Intel/Xeon and Intel/Pentium3 nodes and a SGI Origin2000 numerical server.

3. Results and Discussion

3.1. PES Spectrum. The photoelectron spectra of the anionic UH_2S and UH_2O^7 complexes are much different. The former, however, is very similar to the spectrum of the anionic uracil–glycine (UG) complex,[22] and all three spectra are presented in Figure 4. The spectrum of anionic UH_2O has a maximum at

about 0.9 eV. The spectra of anionic UH$_2$S and UG show broad and structureless features with maxima between 1.7 and 2.1 eV.

The valence π^* and dipole-bound anionic states of uracil are characterized by a calculated value of the VDE of 0.507 and 0.073 eV, respectively.[22] Henceforth, only the valence π^* anionic state will be considered further, since the experimental values of the VDE for UH$_2$A$^-$ are far too large for the dipole-bound anionic state of U$^-$ solvated by H$_2$A. The valence π^* anionic states of uracil, on the other hand, can be involved in the photoelectron spectrum of (UH$_2$O)$^-$, since the solvation of U$^-$ by H$_2$O could easily stabilize U$^-$ by the shift seen in its photoelectron spectrum.

The qualitative difference between the PES spectra of (UH$_2$O)$^-$ and (UH$_2$S)$^-$ poses a challenge for interpretation. The broad photoelectron feature in the (UH$_2$S)$^-$ spectrum with a maximum between 1.7 and 2.1 eV cannot be attributed to U$^-$ in the valence π^* anionic state solvated by H$_2$S. The solvation energy of U$^-$ by H$_2$S would have to be larger than that of U$^-$ by H$_2$O by about 1 eV. This is rather improbable given that H$_2$S both exhibits a lower dipole moment and is a poorer hydrogen bonder than H$_2$O.

We expect that BFPT occurs in anionic complexes of H$_2$S with uracil, in analogy to the anionic UG complexes[22] (see Figure 4). The proton-transfer process to the ring of uracil stabilizes the unpaired electron, which results in larger values of VDE in (UH$_2$S)$^-$ than in (UH$_2$O)$^-$.

3.2. Computational Results. *3.2.1. H$_2$A Monomers.* For H$_2$-Se, H$_2$S, and H$_2$O, the calculated deprotonation energies (E_{DP}), enthalpies (H_{DP}), and Gibbs free energies (G_{DP}) are presented in Table 1 and compared with experimental values. The B3LYP/6-31++G** (5d) values of H_{DP} and G_{DP} for H$_2$Se and H$_2$S are within experimental error bars. The calculated results for H$_2$O are underestimated by ~0.1 eV.

3.2.2. Neutral Complexes. Selenium, sulfur, and oxygen are congeneric elements, and their dihydrides have analogous proton donor and proton acceptor sites. The topological space of the UH$_2$A complexes is limited to four important structures, which are presented for UH$_2$S in Figure 2. Analogous structures were identified for the UH$_2$O and UH$_2$Se complexes.

The important geometrical parameters are presented in Table 2, and stabilization energies and Gibbs free energies, in Table 3. For every A, the largest values of E_{stab} and E_{stab} corrected for zero-point vibrations (E$_{stab}$ + ZPVE) are reported for UH$_2$A$_{O7.N1}$ and the smallest for UH$_2$A$_{O8.C5}$. This is consistent with our previous findings for the neutral complexes of uracil with glycine,[49] alanine,[37] and formic acid.[38] All complexes but UH$_2$O$_{O7.N1}$ are unstable in terms of Gibbs free energy. The stabilization energies of 0.15−0.41 eV are not sufficient to make these complexes thermodynamically stable. It requires an E_{stab} of 0.48 eV for UH$_2$O$_{O7.N1}$ to favor formation of the neutral complex in the gas phase.

For every A, the distance to uracil's oxygen acting as a proton acceptor is shorter for O8 than for O7, which suggests that O8···HA is a stronger hydrogen bond than O7···HA. For every UH$_2$A$_{O8.C5}$ complex, the C5H···A hydrogen bond is longer by more than 0.5 Å than the O8···HA hydrogen bond, which suggests that the former is significantly weaker.

3.2.3. Anionic Complexes. A common feature of anionic wave functions identified by us for the UH$_2$A complexes is that the excess electron is localized on a π^* orbital of uracil, in close resemblance to the valence anionic state of isolated uracil (see Figures 1, 5, and 6). An isolated uracil molecule has a symmetry plane. However, occupation of the antibonding π^* orbital by an excess electron in isolated uracil induces buckling of the

TABLE 2: Bond Distances (Å) for the Neutral and Anionic Complexes[a]

complex	distance	neutral	anion
UH$_2$Se$_{O8.C5}$	SeH···O8	2.192	1.032
	C5H···Se	3.262	3.127
	O8H···Se (BFPT)		2.140
UH$_2$Se$_{O8.N3}$	SeH···O8	2.298	1.023
	N3H···Se	2.875	2.633
	O8H···Se (BFPT)		2.164
UH$_2$Se$_{O7.N1}$	SeH···O7	2.376	1.038
	N1H···Se	2.674	2.484
	O7H···Se (BFPT)		2.119
	SeH···O7[b]		1.748*
	N1H···Se[b]		3.026*
UH$_2$Se$_{O7.N3}$	SeH···O7	2.401	1.741
	N3H···Se	2.793	3.552
UH$_2$S$_{O8.C5}$	SH···O8	2.153	1.051
	C5H···S	3.226	3.050
	O8H···S (BFPT)		1.954
UH$_2$S$_{O8.N3}$	SH···O8	2.217	1.031
	N3H···S	2.789	2.445
	O8H···S (BFPT)		2.013
UH$_2$S$_{O7.N1}$	SH···O7	2.279	1.739
	N1H···S	2.565	3.094
UH$_2$S$_{O7.N3}$	SH···O7	2.281	1.833
	N3H···S	2.708	3.864
UH$_2$O$_{O8.C5}$	OH···O8	1.897	1.707
	C5H···O	2.410	3.252
UH$_2$O$_{O8.N3}$	OH···O8	1.923	1.648
	N3H···O	1.966	2.521
UH$_2$O$_{O7.N1}$	OH···O7	1.942	1.703
	N1H···O	1.927	2.436
UH$_2$O$_{O7.N3}$	OH···O7	1.964	1.777
	N3H···O	1.989	3.150

[a] The results are obtained at the B3LYP/6-31++G**(5d) level. [b] MP2/6-31++G** (5d) results. No BFPT is predicted at this level of theory.

ring because nonplanar structures are characterized by a less severe antibonding interaction. The same kind of ring distortion takes place in all UH$_2$A complexes upon an excess electron attachment.

Our most important finding is that the most stable anionic complexes of U and H$_2$S or H$_2$Se are characterized by a BFPT from the acid to the O8 atom of uracil; see Tables 2 and 3 and Figure 3. A driving force for the proton transfer is to stabilize the excess negative charge, which is primarily localized in the O8−C4−C5−C6 region (see Figures 1, 5, and 6). In consequence of the extra stabilization of the excess electron provided by the transferred proton, the values of VDE for the aUH$_2$-Se$_{O8.C5}$, aUH$_2$Se$_{O8.N3}$, aUH2S$_{O8.C5}$, and aUH2S$_{O8.N3}$ structures are larger by 1.4−1.5 eV than those for the valence anion of an isolated uracil. In fact, the B3LYP/6-3++G** values of VDE for these structures span the ranges 2.18−2.25 eV for aUH$_2$Se and 2.08−2.17 eV for aUH$_2$S, respectively. After correcting the VDEs for aUH$_2$S downward by 0.2 eV, the resulting range 1.88−1.97 eV coincides with a maximum of the photoelectron spectra peak at about 1.9 eV.

For the (UH$_2$O)$^-$ complexes we predict no BFPT from H$_2$O to either O8 or O7 of uracil. The calculated values of VDE for the aUH2O structures span the range 0.96−1.19 eV (0.76−0.99 eV after correcting downward), and they are in good agreement with a maximum of the photoelectron peak at 0.9 eV. Our results are in good agreement with the previous computational results from the group of Ortiz.[17] Another interpretation of the PES spectrum of (UH$_2$O)$^-$ has recently been suggested, which invokes an excess electron being solvated by H$_2$O and uracil.[56] The calculated value of VDE of 0.24 eV[56] is, however, much smaller than the experimental VDE of 0.9 eV.

Effect of Electron Attachment on Proton Transfer

J. Phys. Chem. B, Vol. 107, No. 31, 2003 **7893**

TABLE 3: Thermodynamic Characteristics of the Neutral and Anionic UH$_2$A Complexes and Electron Vertical Detachment Energies (VDEs) for the Anionic Complexes Determined at the B3LYP/6-31++G(5d) Level**[a]

	neutral complexes			anionic complexes				BFPT	
complex	E_{stab}	E_{stab} + ZPVE	G_{stab}	E_{stab}	E_{stab} + ZPVE	G_{stab}	VDE	B3LYP	MPW1K
UH$_2$Se$_{O8.C5}$	0.148	0.096	−0.257	0.924	0.810	0.424	2.248	yes	yes
UH$_2$Se$_{O8.N3}$	0.161	0.116	−0.234	0.974	0.843	0.425	2.178	yes	yes
UH$_2$Se$_{O7.N1}$	0.223	0.170	−0.198	0.606	0.486	0.051	1.700[b]	yes[b]	yes[b]
UH$_2$Se$_{O7.N3}$	0.159	0.106	−0.264	0.359	0.314	−0.035	1.085	no	no
UH$_2$S$_{O8.C5}$	0.155	0.106	−0.225	0.673	0.589	0.210	2.165	yes	yes
UH$_2$S$_{O8.N3}$	0.167	0.116	−0.237	0.749	0.641	0.231	2.083	yes	yes
UH$_2$S$_{O7.N1}$	0.223	0.167	−0.204	0.407	0.351	−0.014	1.048	no	no
UH$_2$S$_{O7.N3}$	0.157	0.107	−0.249	0.378	0.329	0.003	1.065	no	no
UH$_2$O$_{O8.C5}$	0.323	0.243	−0.084	0.652	0.573	0.260	1.188	no	no
UH$_2$O$_{O8.N3}$	0.405	0.311	−0.061	0.643	0.555	0.208	1.100	no	no
UH$_2$O$_{O7.N1}$	0.475	0.376	0.001	0.569	0.474	0.119	0.955	no	no
UH$_2$O$_{O7.N3}$	0.376	0.285	−0.084	0.526	0.441	0.122	1.089	no	no

[a] All energies are in eV. [b] Not confirmed at the MP2 level. The MP2 value of the VDE is 0.56 eV.

aUH$_2$S$_{O8.C5}$
VDE = 2.165 eV

aUH$_2$S$_{O8.N3}$
VDE = 2.083 eV

aUH$_2$O$_{O8.C5}$
VDE = 1.188 eV

aUH$_2$O$_{O8.N3}$
VDE = 1.100 eV

aUH$_2$S$_{O7.N1}$
VDE = 1.048 eV

aUH$_2$S$_{O7.N3}$
VDE = 1.065 eV

aUH$_2$O$_{O7.N1}$
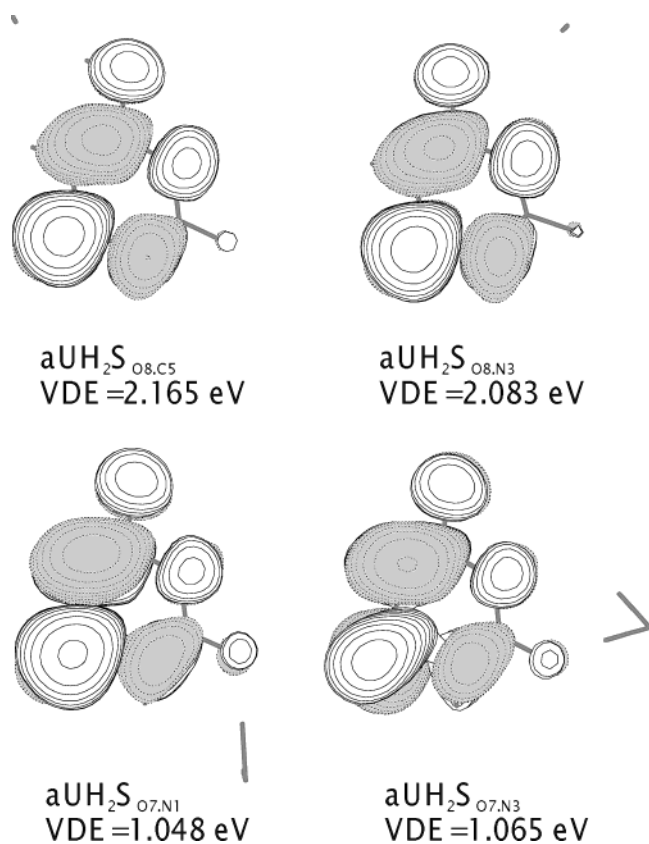VDE = 0.955 eV

aUH$_2$O$_{O7.N3}$
VDE = 1.089 eV

Figure 5. Excess electron orbital for the uracil−H$_2$S complexes. The orbital was plotted with a contour line spacing of 0.02 bohr$^{-3/2}$. The B3LYP/6-31++G** values of electron vertical detachment energies are in eV.

Figure 6. Excess electron orbital for the uracil−H$_2$O complexes. The orbital was plotted with a contour line spacing of 0.02 bohr$^{-3/2}$. The B3LYP/6-31++G** values of electron vertical detachment energies are in eV.

Hence, this interpretation is not supported by our experimental and computational results.

The relative stability is different for the anionic and neutral structures (see Table 3). In general, the anionic complexes of UH$_2$A with a hydrogen bond pointing to O8 of uracil are more stable than those with O7 involved in hydrogen bonding. The difference in the values of G_{stab} for the complexes bound through O8 and O7 is significant for H$_2$Se (0.4 eV) and H$_2$S (0.2 eV) and drops to 0.1 eV for H$_2$O.

Which factors are critical for the occurrence of an intermolecular proton transfer in the (UH$_2$A)$^-$ series? The products of the proton transfer would be the neutral radical UH$^•$ and AH$^-$. The values of H_{DP} and G_{DP} for H$_2$A's are collected in Table 1. The largest protonation enthalpies and Gibbs energies of U$^-$ are at the O8 site (C5 side) and amount to 14.35 and 14.39 eV,
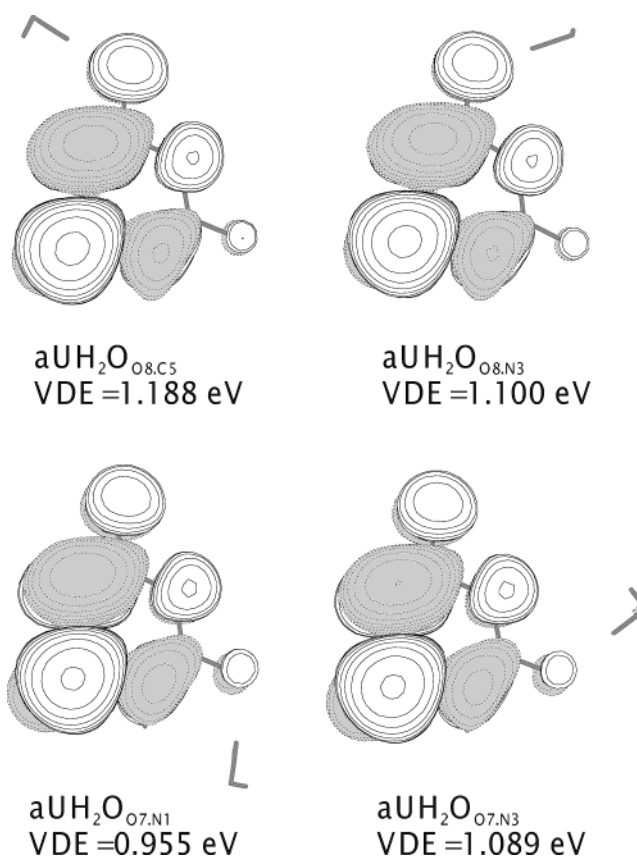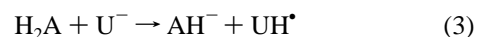
respectively. Hence, a hypothetical process, which leads to noninteracting products

$$H_2A + U^- \rightarrow AH^- + UH^• \qquad (3)$$

is unfavorable in terms of Gibbs free energy by 2.17, 0.45, and 0.12 eV for H$_2$O, H$_2$S, and H$_2$Se, respectively. For the proton transfer to occur, the stabilizing interaction in the UH$^•$···AH$^-$ system needs to (i) compensate the aforementioned barrier and (ii) provide additionally at least as much of the stabilization between the UH$^•$ and AH$^-$ systems as the untransformed U$^-$ and H$_2$A moieties could provide. Indeed, the values of G_{stab} are much larger for the anionic complexes that undergo BFPT (H$_2$A coordinated to the O8 atom (A = Se, S)) than for the

7894 *J. Phys. Chem. B, Vol. 107, No. 31, 2003*

Harańczyk et al.

complexes that do not (see Table 3). The barrier of 2.17 eV for H_2O is too large to be compensated by the interaction between $UH^\bullet$ and OH^-, and the proton transfer does not occur.

The most important geometrical parameters of the anionic UH_2A complexes are presented in Table 2. The dominant hydrogen bond, which involves an oxygen atom of uracil, either undergoes BFPT or does not, but in any case the distance between the proton and the proton acceptor atom (uracil's O or A) is shorter in the anionic than in the neutral complex, which is typical for hydrogen-bonded complexes involving charged species. The second and weaker hydrogen bond ($C5H\cdots A$ or $N1(3)H\cdots A$) is shorter in the anion than in the neutral for these complexes that undergo BFPT and much longer for those complexes that do not. Apparently, the second hydrogen bond stabilizes the $UH^\bullet\cdots AH^-$ complexes, but it does not contribute much to the stability of the $U^-\cdots H_2A$ complexes. The weakening of this bond for the $U^-\cdots H_2A$ complexes must result from the repulsion between the lone electron pair of A and the excess negative charge localized on U. For the $UH^\bullet\cdots AH^-$ complexes, however, the excess negative charge is localized on the AH fragment and the second hydrogen bond, with uracil acting as a proton donor and A as a proton acceptor, becomes stronger than that in the case of neutral complexes.

We performed additional MPW1K/6-31++G** geometry optimizations for all anionic UH_2A complexes considered in this study to validate the B3LYP predictions as to the occurrence of intermolecular proton transfer. The occurrence of BFPT (yes/ no in Table 3) proved to be consistent for the B3LYP and MPW1K functionals. The results for the $aUH_2Se_{O7.N1}$ system were, however, suspicious because in our earlier studies we have never seen a BFPT to the O7 atom of uracil.[22,37,38] Hence, the $aUH_2Se_{O7.N1}$ system was further scrutinized at the MP2 level of theory. In contrast to the B3LYP and MPW1K predictions, the BFPT was not observed at the MP2 level of theory. Moreover, there was no local minimum on the potential energy surface of this anion with the O7 atom protonated. We conclude that the DFT predictions as to the occurrence of BFPT for this conformer are artifacts of currently known exchange-correlation functionals. The MP2 value of VDE for the $aUH_2Se_{O7.N1}$ complex of 0.56 eV is typical for the valence anionic state of U^- weakly solvated by H_2Se through the O7 atom.

4. Conclusions

The photoelectron spectrum of the anionic uracil–H_2S complex has been recorded with 2.540 eV photons. The spectrum reveals a broad feature with its maximum between EBE = 1.7 and 2.1 eV. The vertical electron detachment energy values are too large to be attributed to the anionic complex of an anion of intact uracil solvated by H_2S. The spectrum, on the other hand, is similar to the recently recorded spectrum of the anionic uracil–glycine complex, for which a barrier-free proton transfer was suggested from the carboxylic group of glycine to the anion of uracil.[22] The reported spectrum for the anionic uracil–H_2S differs markedly from the previously recorded spectrum for the anionic uracil–H_2O, which was assigned to the valence anionic state of U^- solvated by H_2O.[7]

The results of density functional calculations with the B3LYP and MPW1K exchange-correlation functionals indicate that an excess electron in the UH_2A (A = Se, S, O) complexes is described by a π^* orbital localized on the ring of uracil. As it was previously observed for complexes of uracil with glycine,[22] alanine,[37] and formic acid,[38] the excess electron can induce a barrier-free proton transfer from H_2Se or H_2S to the O8 atom of uracil. The driving force for the proton transfer is to stabilize

the negative excess charge localized primarily on the O8–C4–C5–C6 fragment of uracil. The barrier-free nature of the proton-transfer process has been confirmed using the MPW1K functional.

The most stable anionic UH_2S complexes undergo BFPT, and the estimated values of VDEs are in the range 1.88–1.97 eV, in agreement with the maximum of the photoelectron spectral peak at 1.9 eV. The occurrence of BFPT is also predicted for the anionic UH_2Se complexes, and the estimated values of VDE are in the range 1.98–2.15 eV. The PES spectrum of the anionic UH_2Se complex has not been measured due to the substantial toxicity of H_2Se. For anionic complexes of U with H_2O, both exchange-correlation functionals predict that the structure with U^- solvated by H_2O is the most stable and BFPT does not occur. The estimated VDE s for these complexes are in the range 0.76–0.99 eV, in good agreement with the measured maximum of the photoelectron peak at 0.9 eV.

Critical factors for the occurrence of BFPT have been analyzed for the anionic UH_2A systems. The reaction $H_2A + U^- \rightarrow AH^- + UH^\bullet$ is unfavorable in terms of Gibbs free energy, with the largest barrier of 2.17 eV for A = O and the smallest of 0.12 eV for A = Se. For the proton transfer to occur, the stabilizing interaction in the $UH^\bullet\cdots AH^-$ system needs to (i) compensate the aforementioned barrier and (ii) provide additionally at least as much of the stabilization between the $UH^\bullet$ and AH^- systems as the untransformed U^- and H_2A moieties could provide. Hence, BFPT does not occur for A = O due to the large barrier of 2.17 eV, but it occurs for A = S and Se.

The relative stability is different for the anionic and neutral structures. The $UH_2A_{O7.N1}$ structure is the most stable for neutral complexes, while the most stable anionic complexes are those with H_2A bound to the O8 atom of uracil. These anionic structures undergo BFPT for A = Se and S, and they do not for A = O. The difference in the values of G_{stab} for anionic complexes bound through O8 and O7 is significant for H_2Se (0.4 eV) and H_2S (0.2 eV) and drops to 0.1 eV for H_2O. The increased stability of anionic complexes that undergo BFPT can be related to the properties of the second hydrogen bond ($C5H\cdots A$ or $N1(3)H\cdots A$). In comparison with the case of neutral structures, this bond is weakened for anionic structures without BFPT and strengthened for those with BFPT.

An important issue for future experimental and theoretical studies is to characterize the propensity of cytosine and thymine to BFPT in anionic complexes with inorganic and organic acids. Last, the formation of neutral radicals of hydrogenated pyrimidine bases may be relevant to DNA and RNA damage by low energy electrons. For instance, the neutral radical $UH^\bullet$, with the O8 atom protonated, cannot form a hydrogen bond with adenine, as dictated by the Watson–Crick pairing scheme. Such a radical might also react with an adjacent deoxyribose molecule, triggering strand-breaks in DNA.

References and Notes

(1) Boudaïffa, B.; Cloutier, P.; Hunting, D.; Huels, M. A.; Sanche, L. *Science* **2000**, *287*, 1658.

Effect of Electron Attachment on Proton Transfer

J. Phys. Chem. B, Vol. 107, No. 31, 2003 **7895**

(2) Burrows, C. J.; Muller, J. G. *Chem. Rev.* **1998**, *98*, 1109.

(3) Armitage, B. *Chem. Rev.* **1998**, *98*, 1171.

(4) Miller, J. H.; Wilson, W. W.; Ritchie, R. H. In *Computational Approaches in Molecular Radiation Biology*; Varma, M. N., Chatterjee, J., Eds.; Plenum Press: New York, pp 65−76.

(5) Michael, B. R.; O'Neill, P. *Science* **2000**, *287*, 1603.

(6) Desfrancois, C.; Carles, S.; Schermann, J. P. *Chem. Rev.* **2000**, *100*, 3943.

(7) Hendricks, J. H.; Lyapustina, S. A.; deClercq, H. L.; Bowen, K. H. *J. Chem. Phys.* **1998**, *108*, 8.

(8) Oyler, N. A.; Adamowicz, L. *J. Phys. Chem.* **1993**, *97*, 11122.

(9) Oyler, N. A.; Adamowicz, L. *Chem. Phys. Lett.* **1994**, *219*, 223.

(10) Roerig, G. H.; Oyler, N. A.; Adamowicz, L. *Chem. Phys. Lett.* **1994**, *225*, 265.

(11) Roerig, G. H.; Oyler, N. A.; Adamowicz, L. *J. Phys. Chem.* **1995**, *99*, 14285.

(12) Smith, D. M. A.; Smets, J.; Elkandi, Y.; Adamowicz, L. *J. Phys. Chem. A* **1997**, *101*, 8123.

(13) Smets, J.; McCarthy, W. J.; Adamowicz, L. *J. Phys. Chem.* **1996**, *100*, 14655.

(14) Smets, J.; Smith, D. M. A.; Elkadi, Y.; Adamowicz, L. *J. Phys. Chem. A* **1997**, *101*, 9152.

(15) Gutowski, M.; Skurski, P. *Recent Res. Dev. Phys. Chem.* **1999**, *3*, 245.

(16) Dolgounitcheva, O.; Zakrzewski, V. G.; Ortiz, J. V. *Chem. Phys. Lett.* **1999**, *307*, 220.

(17) Dolgounitcheva, O.; Zakrzewski, V. G.; Ortiz, J. V *J. Phys. Chem. A* **1999**, *103*, 7912.

(18) Gutowski, M.; Skurski, P.; Simons, J. *J. Am. Chem. Soc.* **2000**, *122*, 10159.

(19) Skurski, P.; Rak, J.; Simons, J.; Gutowski, M. *J. Am. Chem. Soc.* **2001**, *123*, 11073.

(20) Rak, J.; Skurski, P.; Gutowski, M. J. *Chem. Phys.* **2001**, *114*, 10673.

(21) Wesolowski, S. S.; Leininger, M. L.; Pentchev, P. N.; Schaefer, H. F., III. *J. Am. Chem. Soc.* **2001**, *123*, 4023.

(22) Gutowski, M.; Dąbkowska, I.; Rak, J.; Xu, S.; Nilles, J. M.; Radisic, D.; Bowen, K. H., Jr. *Eur. Phys. J. D* **2002**, *20*, 431.

(23) Sevilla, M. D.; Besler, B.; Colson, A. O. *J. Phys. Chem.* **1995**, *99*, 1060.

(24) Lowdin, P. O. *Rev. Mod. Phys*. **1963**, *35*, 724.

(25) Estrin, D. A.; Paglieri, L.; Corongiu, G. *J. Phys. Chem.* **1994**, *98*, 5653.

(26) Morpugo, S.; Bossa, M.; Morpugo, G. O. *Chem. Phys. Lett.* **1997**, *280*, 233.

(27) Kryachko, E. S.; Nguyen, M. T.; Zeegers-Huyskens, T. *J. Phys. Chem. A* **2001**, *105*, 1288.

(28) Kryachko, E. S.; Nguyen, M. T.; Zeegers-Huyskens, T. *J. Phys. Chem. A* **2001**, *105*, 1934.

(29) Hobza, P.; Sponer, J. *Chem. Rev.* **1999**, *99*, 3247.

(30) Dąbkowska, I.; Gutowski, M.; Rak, J. *J. Am. Chem. Soc.*, submitted for publication.

(31) Kim, Y.; Lim, S.; Kim, Y. *J. Phys. Chem. A* **1999**, *103*, 6632.

(32) Bertran, J.; Olivia, A.; Rodriguez-Santiago, L.; Sodupe, M. *J. Am. Chem. Soc*. **1998**, *120*, 8159.

(33) Takeuchi, S.; Tahara, T. *Chem. Phys. Lett.* **1997**, *277*, 340.

(34) Zhanpeisov, N. U.; Sponer, J.; Leszczynski, J. *J. Phys. Chem. A* **1998**, *102*, 10374.

(35) He, F.; Ramirez, J.; Lebrilla, C. B. *J. Am. Chem. Soc.* **1999**, *121*, 4726.

(36) Li, X.; Cai, Z.; Sevilla, M. D. *J. Phys. Chem. A* **2001**, *105*, 10115.

(37) Dąbkowska, I.; Rak, J.; Gutowski, M.; Nilles, J. M.; Radisic, D.; Bowen, K. H., Jr. *J. Chem. Phys.*, submitted for publication.

(38) Haranczyk, M.; Dąbkowska, I.; Rak, J.; Gutowski, M.; Nilles, J. M.; Stokes, S. T.; Radisic, D.; Bowen, K. H., Jr. *J. Phys. Chem. A*, submitted for publication.

(39) Coe, J. V.; Snodgrass, J. T.; Freidhoff, C. B.; McHugh, K. M.; Bowen, K. H. *J. Chem. Phys.* **1987**, *87*, 4302.

(40) Coe, J. V.; Snodgrass, J. T.; Freidhoff, C. B.; McHugh, K. M.; Bowen, K. H. *J. Chem. Phys*. **1986**, *84*, 618.

(41) Hohenberg, P.; Kohn, W. *Phys. Rev.* **1964**, *136*, B864.

(42) Kohn, W.; Sham, L. J. *Phys. Rev.* **1965**, *140*, A1133.

(43) Becke, A. D. *Phys. Rev. A* **1988**, *38*, 3098.

(44) Becke, A. D. *J. Chem. Phys.* **1993**, *98*, 5648.

(45) Lee, C.; Yang, W.; Paar, R. G. *Phys. Rev. B* **1988**, *37*, 785.

(46) Lynch, B. J.; Fast, P. L.; Harris, M.; Truhlar, D. G. *J. Phys. Chem. A* **2000**, *104*, 21.

(47) Ditchfield, R.; Hehre, W. J.; Pople, J. A. *J. Chem. Phys.* **1971**, *54*, 724.

(48) Hehre, W. J.; Ditchfield, R.; Pople, J. A. *J. Chem. Phys.* **1972**, *56*, 2257.

(49) Dąbkowska, I.; Rak, J.; Gutowski, M. *J. Phys. Chem. A* **2002**, *106*, 7423.

(50) Rak, J.; Skurski, P.; Simons, J.; Gutowski, M. *J. Am. Chem. Soc.* **2001**, *123*, 11695.

(51) van Mourik, T.; Price, S. L.; Clary, D. C. *J. Phys. Chem. A* **1999**, *103*, 1611.

(52) Dkhissi, A.; Adamowicz, L.; Maes, G. *J. Phys. Chem. A* **2000**, *104*, 2112.

(53) Rienstra-Kiracofe, J. C.; Tschumper, G. S.; Schaefer, H. F., III. *Chem. Rev.* **2002**, *102*, 231.

(54) Lynch, B. J.; Truhlar, D. G. *J. Phys. Chem. A* **2001**, *105*, 2936.

(55) Frisch, M. J.; et al. Gaussian, Inc.: Pittsburgh, PA, 1998.

(56) Jalbout, A. F.; Hall-Black, C. S.; Adamowicz, L. *Chem. Phys. Lett.* **2002**, *354*, 128.

(57) Stoneman, R. C.; Larson, D. J. *J. Phys. B* **1986**, *19*, 405.

(58) Rempala, K.; Ervin, K. M. *J. Chem. Phys.* **2000**, *112*, 4579.

(59) Schulz, P. A.; Mead, R. D.; Jones, P. L.; Lineberger, W. C. *J. Chem. Phys*. **1982**, *77*, 1153.